Cell

Transcription Factor Achaete Scute-Like 2 Controls Intestinal Stem Cell Fate

Laurens G. van der Flier,[1] Marielle E. van Gijn,[1] Pantelis Hatzis,[1] Pekka Kujala,[2] Andrea Haegebarth,[1] Daniel E. Stange,[1] Harry Begthel,[1] Maaike van den Born,[1] Victor Guryev,[1] Irma Oving,[1] Johan H. van Es,[1] Nick Barker,[1] Peter J. Peters,[2] Marc van de Wetering,[1] and Hans Clevers[1,*]

[1]Hubrecht Institute-KNAW & University Medical Center Utrecht, Uppsalaan 8, 3584 CT Utrecht, The Netherlands

[2]The Netherlands Cancer Institute, Antoni van Leeuwenhoek Hospital, Plesmanlaan 121, 1066 CX Amsterdam, The Netherlands

*Correspondence: clevers@niob.knaw.nl

DOI 10.1016/j.cell.2009.01.031

SUMMARY

The small intestinal epithelium is the most rapidly self-renewing tissue of mammals. Proliferative cells are confined to crypts, while differentiated cell types predominantly occupy the villi. We recently demonstrated the existence of a long-lived pool of cycling stem cells defined by *Lgr5* expression and intermingled with post-mitotic Paneth cells at crypt bottoms. We have now determined a gene signature for these Lgr5 stem cells. One of the genes within this stem cell signature is the Wnt target *Achaete scute-like 2* (*Ascl2*). Transgenic expression of the Ascl2 transcription factor throughout the intestinal epithelium induces crypt hyperplasia and ectopic crypts on villi. Induced deletion of the *Ascl2* gene in adult small intestine leads to disappearance of the Lgr5 stem cells within days. The combined results from these gain- and loss-of-function experiments imply that Ascl2 controls intestinal stem cell fate.

INTRODUCTION

Intestinal crypts contain stem cells and their transit-amplifying (TA) daughter cells. Cells exiting the proliferative crypts onto the villi terminally differentiate into enterocytes, goblet cells and enteroendocrine cells. Paneth cells escape the crypt-villus flow by migrating to crypt bottoms where they live for several weeks. With the exception of stem cells and Paneth cells, the intestinal epithelium is renewed approximately every 5 days (Barker et al., 2008). Proliferation of epithelial crypt cells is Wnt-dependent. Mice that are mutant for an intestine-specific member of the Tcf transcription factor family, *Tcf4*/*Tcf7l2*, fail to establish proliferative crypts during late gestation (Korinek et al., 1998), while conditional deletion of β-catenin (Ireland et al., 2004; Fevr et al., 2007) as well as transgenic expression of the secreted Dickkopf-1 Wnt inhibitor (Pinto et al., 2003; Kuhnert et al., 2004) leads to disappearance of proliferative crypts in adult mice. Moreover, malignant transformation of intestinal epithelium is almost invariably initiated by activating Wnt pathway mutations (Korinek et al., 1997; Morin et al., 1997).

Because of the intimate connection between Wnt signaling and intestinal biology, we have attempted to unravel the TCF4 target gene program activated by this pathway in crypts and colorectal tumors (van de Wetering et al., 2002; van Es et al., 2005; van der Flier et al., 2007). Using Cre-mediated genetic tracing, we demonstrated that Lgr5 marks long-lived, multipotent stem cells (Barker et al., 2007), as predicted originally by Leblond and colleagues (Cheng and Leblond, 1974a, 1974b; Bjerknes and Cheng, 1981a, 1981b, 1999). Each crypt bottom harbours around six of these small, cycling cells intermingled with Paneth cells. Although Lgr5 stem cells occasionally occupy a position directly above the Paneth cells, they are distinct from another proposed stem cell population located at the so called +4 position (Potten et al., 1974, 1977), since Lgr5 stem cells are not particularly radiation-sensitive and do not retain DNA labels (Barker et al., 2007, 2008). Bmi1 expression reportedly also marks cells at position +4. Lineage tracing has revealed that $Bmi1^+$ cells mark pluripotent stem cells that replenish the epithelium with similar kinetics to Lgr5 stem cells (Sangiorgi and Capecchi, 2008). Bmi1 and Lgr5 stem cells may be distinct or may represent overlapping or even identical stem cell populations.

Here, we identify the *Ascl2* gene as one of a few Lgr5 stem cell-enriched genes that were not detected in the immediate daughters. Ascl2 (Mash2/HASH2) is homologous to the *Drosophila* Achaete-scute complex genes (Johnson et al., 1990). *Ascl2* expression in the intestinal epithelium is Wnt-dependent (Sansom et al., 2004; Jubb et al., 2006; van der Flier et al., 2007). The *Ascl2* gene encodes a basic helix-loop-helix (bHLH) transcription factor with an unusually restricted expression pattern, *i.e.* its expression is predominantly detected in extraembryonic tissues (Guillemot et al., 1994) and in intestinal epithelium (see below). $Ascl2^{-/-}$ embryos die from placental failure around 10.5 days post-coitum, when the spongiotrophoblasts lineage is depleted and the number of giant cells is elevated (Guillemot et al., 1994). Here we demonstrate an essential role for Ascl2 in the maintenance of adult intestinal stem cells.

RESULTS

Intestinal Stem Cell Transcriptome

We sorted GFP-positive epithelial cells from isolated crypts of *Lgr5-EGFP-ires-CreERT2* mice (see Experimental Procedures). FACS analysis distinguished a GFP-high (GFP^{hi}) and a GFP-low (GFP^{lo}) population (Figure 1A), which we tentatively identified as Lgr5 stem cells and their immediate transit-amplifying daughters, respectively. A single mouse intestine routinely yielded

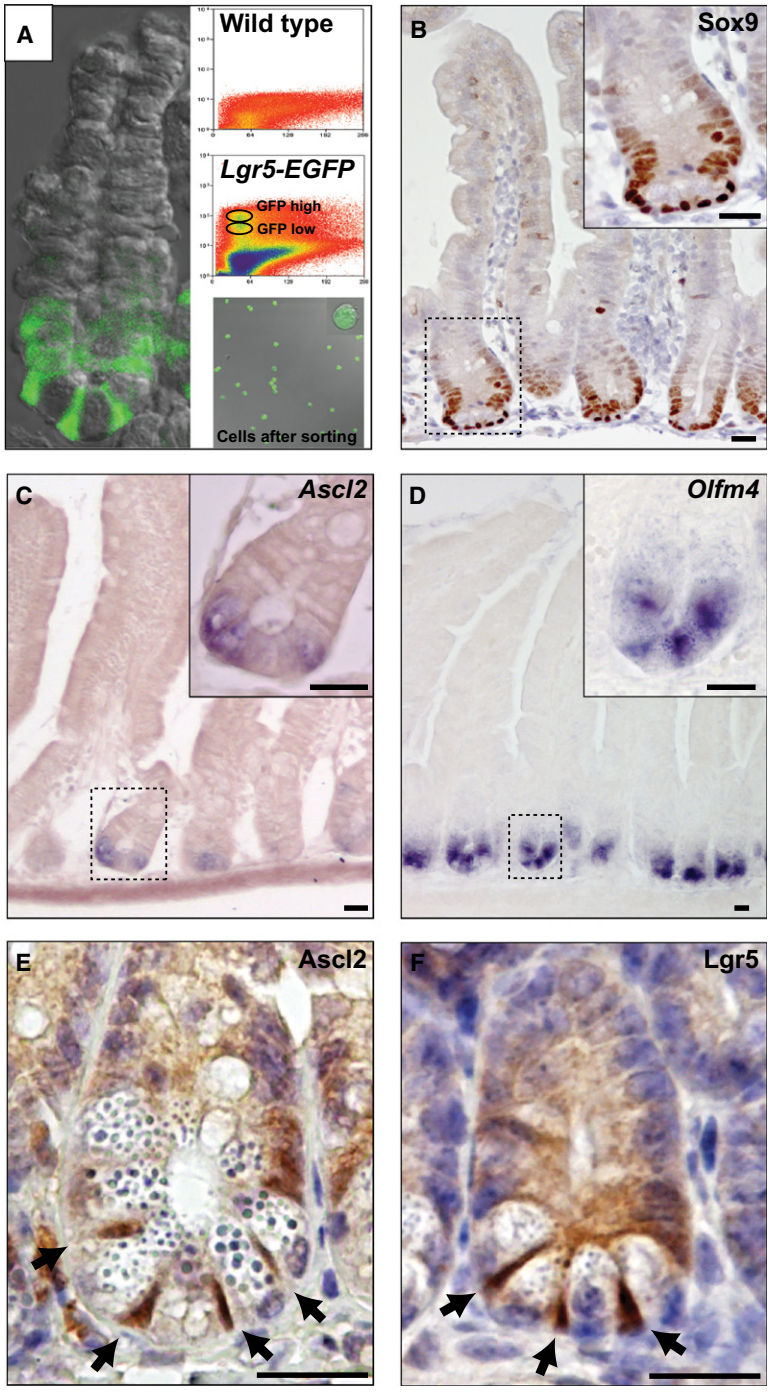

Figure 1. Ascl2, *Olfm4*, and Lgr5 as Intestinal Stem Cell Markers

(A) Confocal images of an isolated *Lgr5-EGFP-ires-CreERT2* crypt (left). After treatment with trypsine, GFP^{hi} and GFP^{lo} cells were identifiable upon sorting (right/middle) when compared to wild-type crypt cells (right/top). Confocal image of healthy sorted GFP^{hi} cells (right/bottom).

(B) Sox9 antibody staining shows high level expression in Lgr5 stem cells and Paneth cells. TA cells directly above the Paneth cells also express the gene, albeit at a much lower level.

(C) In situ hybridization for *Ascl2* reveals an Lgr5 stem cell-restricted expression pattern.

(D) In situ hybridization for *Olfm4* reveals an Lgr5 stem cell-restricted expression pattern.

(E) Monoclonal Ascl2 antibody stains nuclei of Lgr5 stem cells (arrows). Neither the surrounding post-mitotic Paneth cells at the crypt base, nor the TA cells show any positive signal. Hematoxylin is used as a counter stain to visualize Paneth cell granules.

(F) Cytoplasmic GFP staining in *Lgr5-EGFP-ires-CreERT2* knock-in mice reveals Lgr5 stem cells (arrows). Hematoxylin is used as a counter stain.

Scale bars represent 20 μm.

several hundred thousand GFP^{hi} and GFP^{lo} cells. mRNA samples were subjected to comparative gene expression profiling. A comprehensive list of Lgr5 stem cell genes is given in Table S1 (available with this article online). The gene that was most highly enriched in the GFP^{hi} cells was, satisfactorily, the *Lgr5* gene itself. Multiple genes on the list were already identified as intestinal Wnt target genes previously (van der Flier et al., 2007) (Table S1). While in situ hybridizations on these Wnt target genes typically confirmed high level expression in Lgr5 stem cells, TA cells directly above the Paneth cells often also expressed these genes, albeit at a lower level. As an example, Figure 1B shows the expression of *Sox9*, a Wnt-responsive gene (Blache et al., 2004) crucial for Paneth cell specification (Bastide et al., 2007; Mori-Akiyama et al., 2007).

Ascl2 was one of the known Wnt target genes (Sansom et al., 2004; Jubb et al., 2006; van der Flier et al., 2007) and was expressed in adenomas as expected (Figures S1A, S1D, and S1E). Its physiological expression, however, was restricted to cells at the base of crypts as revealed by in situ hybridization (Figure 1C). In situ hybridization analysis also identified *Olfactomedin-4* (*Olfm4*) as a highly-specific and robust marker for Lgr5 stem cells (Figure 1D). *Olfm4* was not expressed under the control of Wnt, since it was absent from adenomas (Figure S1B). Human *OLFM4* is enriched in human colon crypts (Kosinski et al., 2007). OLFM4 is a secreted molecule originally cloned from human myeloblasts (Zhang et al., 2002). Recently, it was shown that *Xenopus* ONT1, an Olfm family member, acts as a BMP antagonist (Inomata et al., 2008).

To study the expression pattern of Ascl2 more precisely we generated monoclonal antibodies against the C-terminal part of the mouse Ascl2 protein. The mouse Ascl2 protein was detected in E10.5 spongiotrophoblasts cell nuclei by immunohistochemistry (IHC) (Figure S1C). In the intestine, Ascl2 was found to be expressed in slender cells with the unique morphology and location of Lgr5 stem cells (Figure 1E), yet was not expressed in Paneth cells or the transit-amplifying cells. Figure 1F compares Ascl2 nuclear staining to cytoplasmic GFP in *Lgr5-EGFP-ires-CreERT2* knock-in intestine. Ascl2 was expressed by the Lgr5 stem cells

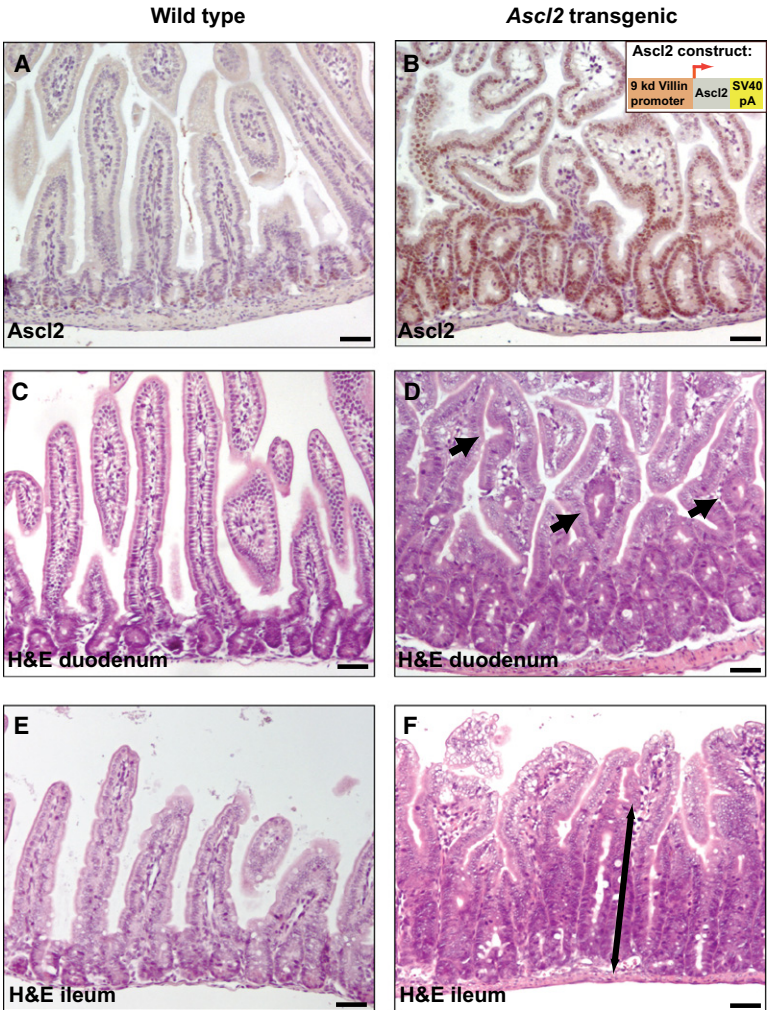

Figure 2. Intestine-Specific Ascl2 Misexpression

(A) Monoclonal Ascl2 antibody staining reveals Lgr5 stem cell-restricted Ascl2 expression in wild-type animals.

(B) In *villin-Ascl2*-transgenic animals, epithelial nuclei along the crypt-villus axis stain for Ascl2. Insert outlines the transgene construct.

(C) H&E staining showing normal crypt-villus morphology in the duodenum of wild-type animals.

(D) H&E staining showing aberrant epithelium morphology in the duodenum of transgenic animals. Villi are branched and display crypt-like pockets (arrows).

(E) H&E staining showing normal crypt-villus morphology in the ileum of wild-type animals.

(F) H&E staining showing elongated crypts (arrow), with short, disorganized villi in the ileal epithelium of *Ascl2* transgenics. Scale bars represent 50 μm.

at the crypt base as revealed by serial sectioning (Figures S1F and S1G).

GFP^{hi} and GFP^{lo} cells from duodenum, ileum and colon of *Lgr5-EGFP-ires-CreERT2* mice were subjected to real-time qPCR analysis. This confirmed that Lgr5, Ascl2, Tnfrsf19 and Olfm4 were highly enriched in stem cells of the small intestine (Figure S1H). Only Lgr5 and Ascl2 were enriched in the GFP^{hi} stem cells of the colon. Expression of Bmi1, another putative stem cell marker, was readily detected in all fractions and was slightly enriched in GFP^{hi} stem cells of the small intestine, albeit to a lesser extent than Lgr5 or Ascl2. We then tested intestines from 4 week-old *Bmi1* null animals (van der Lugt et al., 1994) for stem cell marker gene expression. Histologically and by marker analysis, the intestinal epithelium of these mutant mice was indistinguishable from wild-type littermates (van Lohuizen and Clevers, unpublished). Both, Ascl2 and *Olfm4* were expressed in the intestines of these animals (Figures S1I and S1J).

Consultation of adult man and mouse EST data sets using the Unigene database (http://www.ncbi.nlm.nih.gov/sites/entrez?db=unigene&cmd=search&term=) indicated that *Ascl2* is expressed uniquely in the small intestine and colon.

Transgenic Expression of Ascl2

We generated transgenic mice expressing a mouse *Ascl2* cDNA under the control of the villin promoter (insert in Figure 2B). This promoter drives expression throughout the intestinal epithelium and becomes fully active during late gestation (Pinto et al., 1999). Four independent transgenic mice were born. Three of these showed growth retardation and were sacrificed within 2-3 weeks postnatally. The founder of the fourth line was healthy and fertile, yet yielded multiple litters which contained transgenic F1 offspring at Mendelian ratios. These transgenic F1 individuals displayed the same phenotype as the three other independent transgenic mice. This fortunate situation allowed us to study the phenotype of the fourth transgenic line and to confirm the observations using fixed material from the three independent transgenic mice.

Transgenic animals were analyzed at P14 when they were still relatively healthy, yet had already replaced their postnatal intervillus pockets by adult-type crypts (Gregorieff and Clevers, 2005). Nuclear Ascl2 was observed throughout crypt and villus epithelium (Figures 2A and 2B). H&E histology revealed dramatic changes in the transgenic epithelium. In the duodenum, villi were branched and displayed crypt-like pockets (Figures 2C and 2D). In the ileum, crypts were elongated (“hyperplastic”), while villi were short and disorganized (Figures 2E and 2F). Ki67 staining revealed that proliferation in the Ascl2 transgenic intestines occurred in pockets along the villi (Figures 3A and 3B) which also expressed the Wnt target gene *cMyc* (Figures 3E and 3F). *Ets2*, a Wnt target gene specifically expressed at the crypt base (van de Wetering et al., 2002) and enriched in Lgr5 stem cells (Table S1) was strongly expressed in the elongated crypts and villi (Figures 3I and 3J). The expression domains of the *Olfm4* and *Lgr5* genes were expanded in the hyperplastic ileal crypts (Figures 3C, 3D, 3G, and 3H), as was the expression domain of the *Sox9* gene (Figures 3K and 3L).

In the fly, the *achaete-scute* gene products form heterodimers with the Daughterless protein (Cabrera and Alonso, 1991; Caudy et al., 1988). In a yeast 2-hybrid assay using ASCL2 as bait on

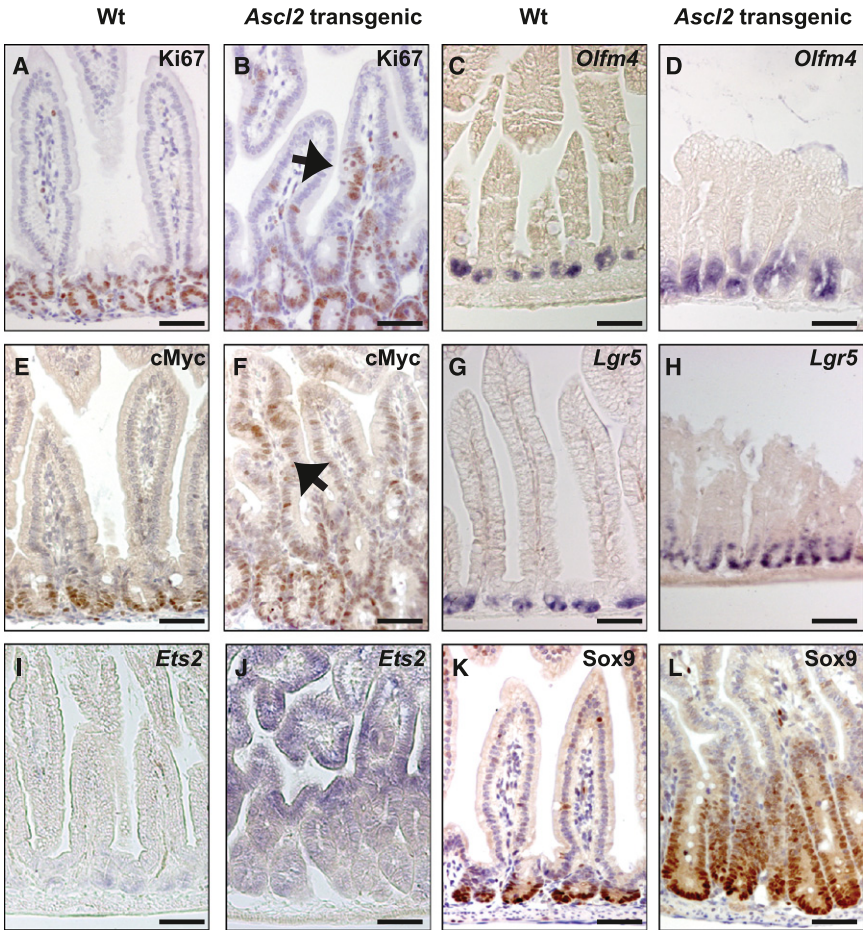

Figure 3. Marker Analysis in the Villin-Ascl2 Intestine

Marker analysis of intestinal epithelium in wild-type (A, C, E, G, I, and K) and *Ascl2*-transgenic (B, D, F, H, J, and L) animals.

(A and B) Ki67 analysis shows aberrant (arrow), dividing regions along the villus epithelium of *Ascl2* transgenic animals.

(C and D) In situ hybridization for the Lgr5 stem cell marker *Olfm4* shows increased signal in the hyperplastic ileal crypts of *Ascl2* transgenics.

(E and F) The aberrant dividing regions along the villus epithelium of *Ascl2* transgenics are also positive for the crypt marker cMyc (arrow).

(G and H) In situ hybridization for stem cell marker *Lgr5* shows elevated expression in the hyperplastic ileal crypts.

(I and J) In situ hybridization for the crypt marker *Ets2* show that the expression in *Ascl2* transgenic animals is found along the entire crypt-villus axis.

(K and L) IHC Staining for the crypt marker Sox9 shows expanded expression of this protein in the hyperplastic crypts of *Ascl2* transgenic animals.

Scale bars represent 50 μm.

a human colon library, we predominantly found the nuclear proteins E22, E2A and HEB as ASCL2-binding partners confirming previous observations (Johnson et al., 1992; Scott et al., 2000). These three common E-proteins are the homologs of Daughterless. *E2a* and *Heb* were expressed in crypts and adenomas (Figures S2A and S2B). The crypt-restricted expression of these co-factors explained why the transgenic overexpression of Ascl2 only partially affected the villus epithelium.

Generation of a Conditional *Ascl2* Allele

As *Ascl2*$^{-/-}$ animals die around E10.5 (Guillemot et al., 1994), we generated a conditional *Ascl2* allele (Figure S3A). The murine *Ascl2* gene contains three exons of which the middle exon encodes the protein. We introduced LoxP sites into 5′ UTR of exon I and in intron II. Cre-mediated recombination should result in a null allele. The paternal *Ascl2* allele is silenced during postimplantation development (Guillemot et al., 1995). By utilizing the LoxP site in exon I as an allele-specific marker, we found that both alleles of *Ascl2* were expressed in the mouse intestine (Figure S3B). We crossed the floxed animals with the *Ah-Cre* mouse (Ireland et al., 2004) in which expression of *Cre* is driven by the *Cyp1a* promoter, inducible in a number of tissues by β-Naphtoflavone (ßNF). The resulting gene deletion in the intestinal epithelium is highly efficient, includes the intestinal stem cells and remains stable over many months (Ireland et al., 2004). A dramatically different observation was made when we deleted the functionally important *c-Myc* gene using the same protocol (Muncan et al., 2006). The epithelium, which was essentially c-Myc$^{-/-}$ at day 4 post-induction (PI), was entirely replaced by wild-type epithelium derived from low numbers of escaping, nondeleted cells within 2-3 weeks.

We analyzed adult *Ah-Cre*/*Ascl2*$^{floxed/floxed}$ animals at 5, 8, 11 and 15 days PI and compared these to ßNF-treated *Ascl2*$^{floxed/floxed}$ litter mates. Intestinal epithelium was subjected to Southern blot analysis (Figure S3A). Figure 4A (upper panel) shows recombination of the *Ascl2*$^{floxed/floxed}$ locus at the indicated days PI. Complete recombination was observed at the 5- and 8-day time points. At 11 days PI, a partial return of nonrecombined alleles was observed. At day 15, recombined alleles were no longer observed. The rapid reappearance of wild-type epithelium implied a strong selective pressure favoring the few remaining Ascl2^{+} epithelial Lgr5 stem cells. The *Ah-Cre* transgene is also inducible in the liver, albeit to a lesser extent (Ireland et al., 2004). As the *Ascl2* gene is not expressed in liver, its deletion should be neutral in terms of selection. A significant, albeit not entirely complete, deletion of the *Ascl2* gene was observed in liver (Figure 4A, lower panel). This deletion pattern remained unchanged over time. Quantitative recombination was confirmed through Northern blot analysis of intestinal epithelial extracts (Figure 4B) and Ascl2 antibody stainings (Figures 4C–4G).

To directly visualize the rescue process, we bred the Cre-activatable *Rosa26-LacZ* reporter (Soriano, 1999) into the *Ah-Cre*/*Ascl2*$^{floxed/floxed}$ strain. *Rosa26-LacZ*/*Ah-Cre*/*Ascl2*$^{floxed/floxed}$ animals were treated with ßNF and intestines were isolated at 5, 10 or 20 days PI. Intestines of *Rosa26-LacZ*/*Ah-Cre*/*Ascl2*$^{floxed/wt}$ animals were used as controls. Figures 4H–4K illustrates LacZ

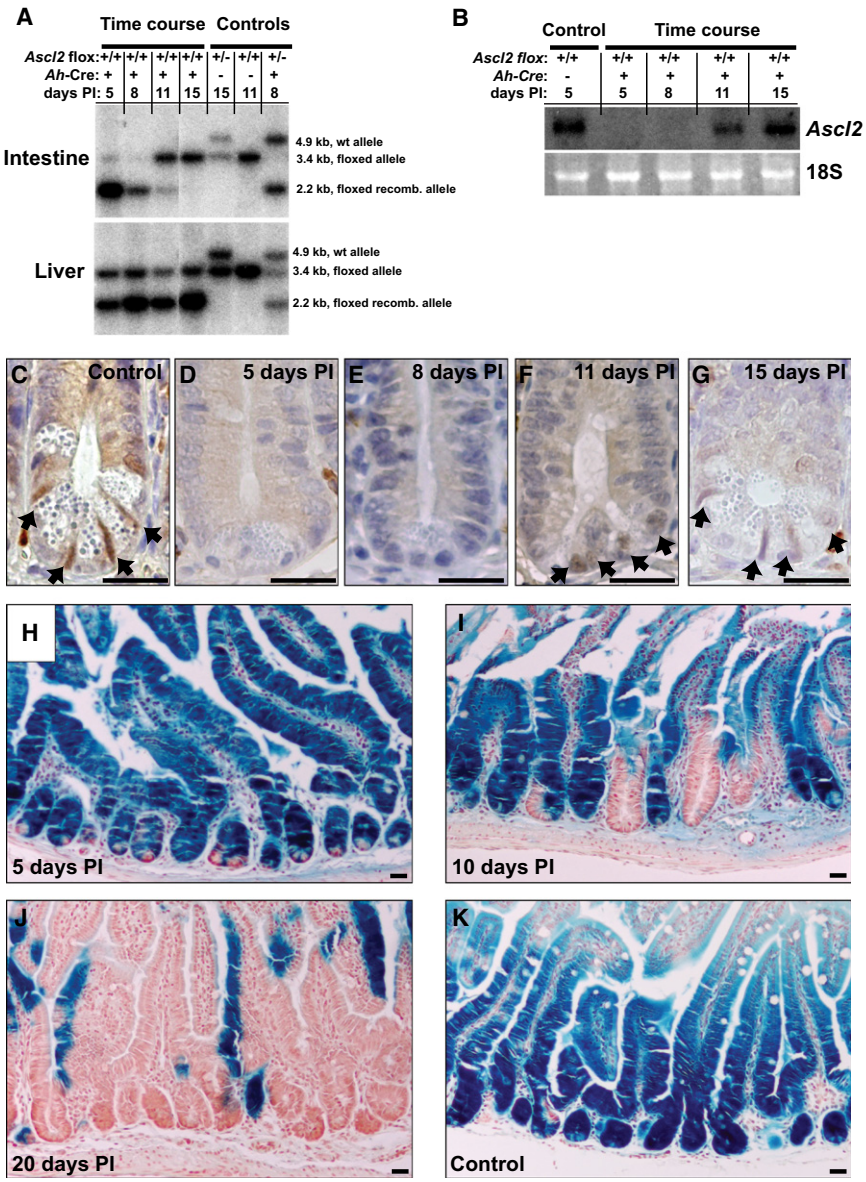

Figure 4. Conditional *Ascl2* Inactivation in the Intestinal Epithelium

(A) Southern blot analysis of genomic DNA of intestinal epithelial cell extracts (upper panel) and liver samples (lower panel) of *Ah-Cre/Ascl2*$^{floxed/floxed}$ animals 5, 8, 11, and 15 days PI and control animals. DNA was digested with EcoRV and hybridized with probe A (as indicated in Figure S3A).

(B) *Ascl2* Northern blot analysis on total RNA from intestinal epithelial cell extracts of *Ah-Cre/Ascl2*$^{floxed/floxed}$ animals 5, 8, 11, and 15 days PI and control.

(C–G) Monoclonal Ascl2 antibody staining demonstrates Lgr5 stem cell restricted expression of the Ascl2 protein (arrows) in control animals (C). 5 (D) and 8 (E) days PI the Ascl2 signal is completely gone. The signal reappears in the Lgr5 stem cells 11 (F) and 15 (G) days PI.

(H–K) LacZ staining of the duodenum illustrates recombination efficiency in *Rosa26-LacZ/Ah-Cre/Ascl2*$^{floxed/floxed}$ animals 5, 10 and 20 days PI. At 5 days PI, virtually all cells were recombined (blue) except for long-lived Paneth cells (H). At 10 days PI, nonrecombined epithelial cells started reappearing (I). At 20 days PI, virtually all crypts were wild-type (J). In *Rosa26-LacZ/Ah-Cre/Ascl2*$^{floxed/wt}$ control animals 20 days PI, the entire intestinal epithelium remained blue (K).

Scale bars represent 25 μm.

staining of the duodenum. At 5 days PI, virtually all cells were recombined and blue except for long-lived Paneth cells (Figure 4H). At 10 days PI, nonrecombined epithelial cells started reappearing (Figure 4I). At 20 days PI, virtually all crypts were again wild-type (Figure 4J). In heterozygous intestines at 20 days PI, the entire epithelium stained blue (Figure 4K).

Intestinal Stem Cells Are Lost upon Conditional Deletion of *Ascl2*

No dramatic histological differences were observed by H&E staining (Figures 5A and 5B) or Ki67 staining (Figures 5C and 5D) at 5 days PI. The crypt base entirely consisted of Paneth cells, while Lgr5 stem cells recognizable by their elongated Ki67^{+} nuclei were conspicuously absent (Figures 5C and 5D). These observations were confirmed by electron microscopy (Figures S4A and S4B). There was an increase in apopototic cells in the crypts of floxed animals (Figures 5E and 5F). Analysis at late time points PI revealed a strong increase in crypt fission profiles (Figures 5G and 5H). Crypt fission represents a powerful repair mechanism of the intestinal epithelium, for instance after radiation injury or genetic damage (Cairnie and Millen, 1975; Muncan et al., 2006).

To follow the fate of Lgr5 stem cells more precisely, we utilized the robust Olfm4 marker. In situ hybridizations for *Olfm4* expression confirmed that the *Olfm4*$^{+}$ Lgr5 stem cells were present in every single crypt of control intestines (Figure 6A). Five days PI, *Olfm4*$^{+}$ Lgr5 stem cells had vanished (Figure 6B). At day 8 PI, an *Olfm4* signal reappeared in occasional crypts (Figure 6C). By 11 days PI (Figure 6D), larger patches of *Olfm4*$^{+}$ crypts reappeared. By day 15 PI, all crypts were *Olfm4*$^{+}$ (Figure 6E).

To investigate the target gene program regulated by Ascl2 in the small intestine, we performed comparative gene expression profiling on RNA samples from isolated intestinal epithelium of *Ah-Cre/Ascl2*$^{floxed/floxed}$ animals and *Ah-Cre/Ascl2*$^{floxed/wt}$ control animals at day 3 and 5 days PI. A total of 130 genes, also expressed by Lgr5 stem cells, was significantly downregulated > 1.5-fold at both time points PI. Comparison of these Ascl2 target genes with the stem cell gene signature (Table S1) revealed a ~25% overlap (Figure 7A; Table S2).

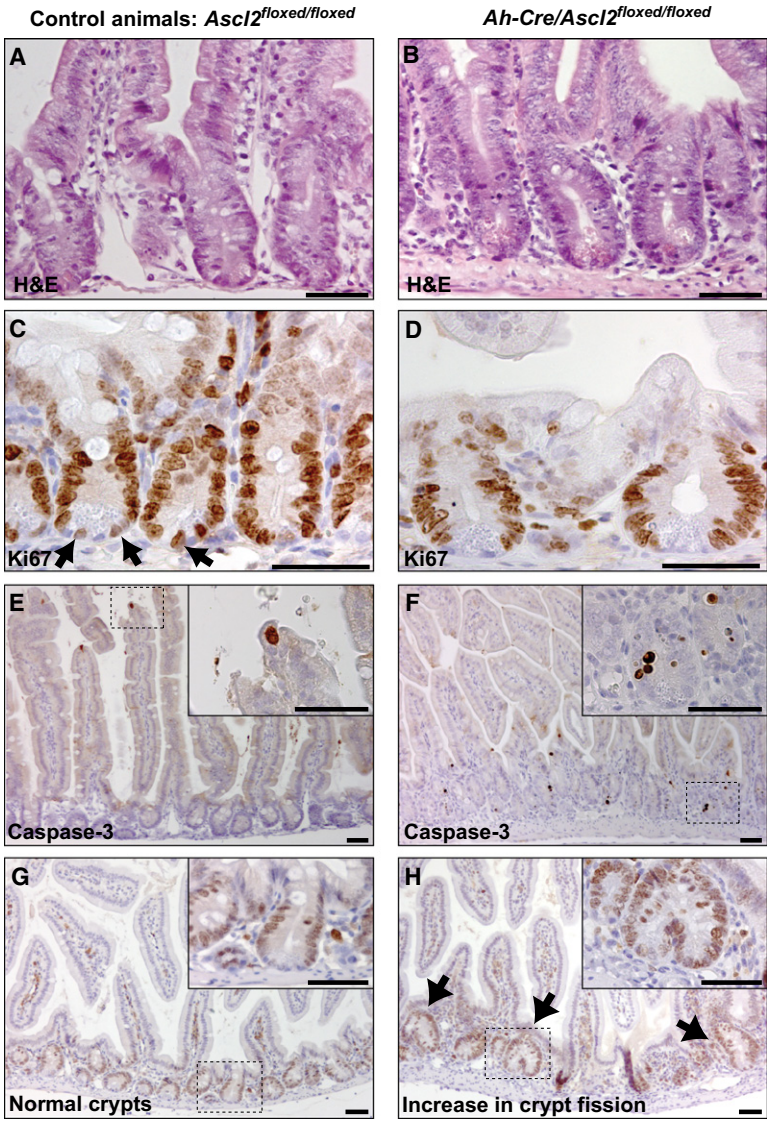

Figure 5. Expansion of Ascl2 Wild-Type Crypts through Crypt Fission

(A and B) H&E staining reveals normal morphology of crypt-villus epithelium of *Ascl2*$^{floxed/floxed}$ control animals (A) and *Ah-Cre/Ascl2*$^{floxed/floxed}$ animals 5 days PI (B).

(C and D) Ki67 staining showing normal numbers of proliferating cells in intestinal crypts of *Ascl2*$^{floxed/floxed}$ control animals (C) and *Ah-Cre/Ascl2*$^{floxed/floxed}$ animals 5 days PI (D).

(E and F) Active Caspase-3 staining showing apoptosis predominantly at the villus tip in *Ascl2*$^{floxed/floxed}$ control animals (E). At 5 days PI, a strong increase in apoptosis in the crypt region of *Ah-Cre/Ascl2*$^{floxed/floxed}$ animals can be observed (F).

(G and H) Ki67 staining showing at a low magnification, normal crypt-villus epithelium in *Ascl2*$^{floxed/floxed}$ control animals (G). An increase in crypt fission (arrows) in *Ah-Cre/Ascl2*$^{floxed/floxed}$ animals 11 days PI is observed (H).

Scale bars represent 50 μm.

To identify in vivo ASCL2 binding sites, we performed chromatin immunoprecipitations (ChIP) on human LS174T colorectal cancer (CRC) cells. We probed a customized array containing a set of TCF4-regulated genes (Hatzis and Clevers, unpublished). Potential ASCL2-bound regulatory regions were verified by qPCR. LGR5, EPHB3 and TNFRSF19 promoters were bound by ASCL2, while the OLFM4 promoter was not. Nonpromoter sequences in the PTPRO, SOAT1, ETS2 and SOX9 loci were also bound by ASCL2 (Figure 7B).

As a further validation of these data, we created an LS174T transfectant carrying a stably integrated, doxycycline-inducible sh-RNA expression vector targeting ASCL2. An essentially complete knock-down of the ASCL2 mRNA occurred within 24 hr upon RNAi induction, as shown by Northern blot analysis (Figure S5A). We used this cell line to validate the generated ChIP signals. As can be seen in Figure S5B, the ChIP signals for the EPHB3 promoter and the ETS2 enhancer disappeared upon ASCL2 knock-down. We cloned the putative *SOX9* enhancer in a luciferase reporter plasmid. Transient transfection was performed in the inducible LS174T ASCL2 RNAi cell line. Figure 7C shows that the spontaneous activity of the *SOX9* enhancer was significantly downregulated upon ASCL2 knock-down. For the reverse experiment, we stably integrated a dox-inducible ASCL2 expression plasmid into HCT116 cells. This CRC cell line does not express endogenous ASCL2 (Figure S5C). Transient transfection of the *SOX9* enhancer plasmid in this cell line resulted in a significant activation of the *SOX9* enhancer upon ASCL2 induction (Figure 7D).

We interpreted the combined observations in the following manner. The *Ascl2* gene is crucial for the maintenance of Lgr5 stem cells, the only cells in the intestine that express the gene. Part of the stem cell signature is Ascl2-dependent and involves binding of Ascl2 to promoters and/or enhancers elements to activate transcription of these target genes. In the absence of Ascl2 expression, Lgr5 stem cells rapidly disappear. *Ascl2* deletion in TA cells does not directly harm these cells as they normally don't express the gene. The mutant TA cells continue to proliferate and provide the villi with differentiated cells. However, no new TA cells are produced from Lgr5 stem cells in mutant crypts. The strong increase in apoptosis in the TA compartment likely mirrors the limited self-renewal capacity that these cells possess. As a consequence, a strong selective pressure is exerted which favors the re-emergence of "escaper" crypts harboring intact *Ascl2* alleles.

DISCUSSION

Here, we define a minimal gene expression profile for the Lgr5 stem cells. Lgr5 is the most differentially expressed gene within this set. Many other genes in the signature represent previously identified Wnt-dependent genes, e.g., *Ascl2, CD44, Ephb3* and *Sox9* (van der Flier et al., 2007). Given the intimate connection between Wnt signaling and the biology of stem cells (Reya and

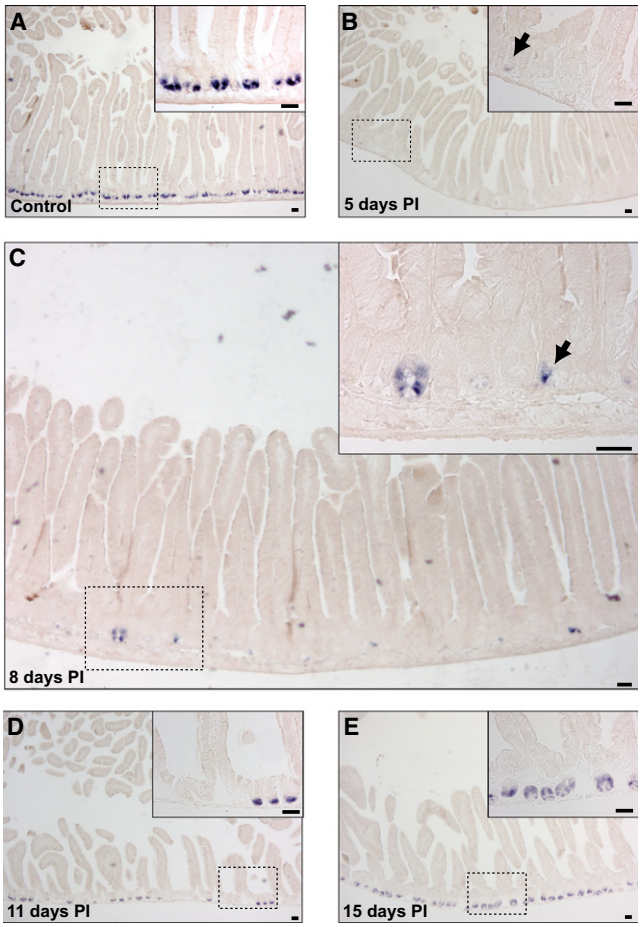

Figure 6. Intestinal Stem Cells Are Lost upon Ascl2 Deletion

Olfm4 in situ hybridizations to visualize Lgr5 stem cells in *Ah-Cre/Ascl2*$^{floxed/floxed}$ small intestines 5, 8, 11 and 15 days PI and in a control intestine.

(A) *Olfm4* in situ staining at low magnification shows Lgr5 stem cell specific staining in *Ascl2*$^{floxed/floxed}$ control animals in every crypt.

(B) The *Olfm4* signal is almost completely gone 5 days PI in *Ah-Cre/Ascl2*$^{floxed/floxed}$ animals. Sporadic positive Lgr5 stem cells can be observed (arrow).

(C) Eight days PI most of the crypts are still negative for *Olfm4*, although sporadic crypts display normal staining, while other crypts contain 1 or 2 positive Lgr5 stem cells (arrow).

(D) At 11 days PI, the tissue of *Ah-Cre/Ascl2*$^{floxed/floxed}$ shows patches of positive and patches of negative crypts for *Olfm4*.

(E) The *Olfm4* signal is completely restored 15 days PI in the *Ah-Cre/Ascl2*$^{floxed/floxed}$ *animals*.

Scale bars represent 50 μm.

Clevers, 2005), this was not surprising. At least one novel marker for Lgr5 stem cells, *Olfm4*, was not expressed under the control of the Wnt pathway, implying the existence of a Wnt-independent specifier for stem cell identity.

Ascl2 is one of the mammalian homologous of the *Drosophila achaete-scute* complex genes (Johnson et al., 1990). This complex encodes related bHLH proteins that are powerful regulators of cell fate. The *achaete-scute* genes are initially expressed in proneural cell clusters were they promote neuroblast differentiation. They are essential for the differentiation of the central as well as peripheral nervous system (Calleja et al., 2002). *Achaete-scute* genes are best known as targets of the Notch pathway. *Hairy/Enhancer of Split* genes, activated by Notch signaling, directly repress the proneural *achaete-scute* genes. The indirect repression by Notch signals allows *achaete-scute* gene-expressing cells to be singled-out through lateral inhibition (Simpson, 1990). However, *achaete-scute* genes can also be expressed under control of the Wnt pathway. Wingless expression is required for *achaete-scute* complex gene expression along the wing margin and for *achaete-scute*-dependent formation of margin bristles and their precursors (Phillips and Whittle, 1993). Intestinal *Ascl2* is expressed under the control of the Wnt pathway. In a recent genome-wide TCF4 Chromatin Immunoprecipitation study, we have observed that the *ASCL2* locus in human CRC cells contains two TCF4/β-catenin-bound regulatory elements, indicating that ASCL2 is a direct target of the Wnt pathway (Hatzis et al., 2008).

Like its fly counterparts, mammalian Ascl2 appears to control lineage specification. In *Ascl2*-mutant mice, the spongiotrophoblast layer is lost by embryonic day E10 at the expense of trophoblast giant cells (Guillemot et al., 1994; Hughes et al., 2004). The current study demonstrates that *Ascl2* is essential for the maintenance of Lgr5 stem cells in the adult intestinal epithelium and that misexpression of *Ascl2* in nonstem cells results in crypt hyperplasia and crypt-like pockets on villi. In conclusion, we have initiated a molecular characterization of the stem cell of the intestinal epithelium by gene expression profiling of essentially pure Lgr5 stem cells. The current study of Ascl2 demonstrates that, with the available genetic tools, the intestinal epithelium constitutes a prime model to unveil molecular mechanisms underlying the biology of stem cells.

EXPERIMENTAL PROCEDURES

Isolation of GFP-Positive Epithelial Cells

Freshly isolated small intestines were incised along their length and villi were removed. The intestinal tissue was washed in PBS/EDTA (5 mM) for 5 min, and subsequently incubated in fresh PBS/EDTA for 30 min at 4°C. Vigorous shaking yielded free crypts which were incubated in PBS supplemented with Trypsine (10 mg/ml) and DNase (0.8 u/μl) for 30 min at 37°C. After incubation, cells were spun down, resuspended in SMEM (Invitrogen) and filtered through a 40 μm mesh. GFP-expressing cells were isolated using a MoFlo cell sorter (DAKO).

Microarray Analysis

RNA was isolated from sorted GFP^{hi} and GFP^{lo} cell fractions of intestines from *Lgr5-EGFP-ires-CreERT2* mice. For the analysis of Ascl2 target genes, RNA was isolated from intestinal epithelial cells of *Ah-Cre/Ascl2*$^{floxed/floxed}$ animals and *Ah-Cre/Ascl2*$^{floxed/wt}$ control animals 3 and 5 days post Cre induction. 500 ng of total RNA was labeled using low RNA Input Linear Amp kit (Agilent Technologies, Pato Alto, CA, USA). Labeling, hybridization, and washing protocols were done according to Agilent guidelines. Detailed information is available in Supplemental Experimental Procedures.

Mice

The *villin-Ascl2* transgenic expression construct was generated by cloning the mouse Ascl2 coding sequence at the initiation codon of the 9-kb regulatory region of the mouse *villin* gene (Pinto et al., 1999). An SV40 termination and polyadenylation cassette was added downstream (Figure 2B, insert). Conditional *Ascl2* mice were generated through homologous recombination in embryonic stem cells as depicted in Figure S3A. More detailed information is available in Supplemental Experimental Procedures. The transgenic *Ah-Cre* line (Ireland et al., 2004) was crossed with conditional Ascl2 mice to

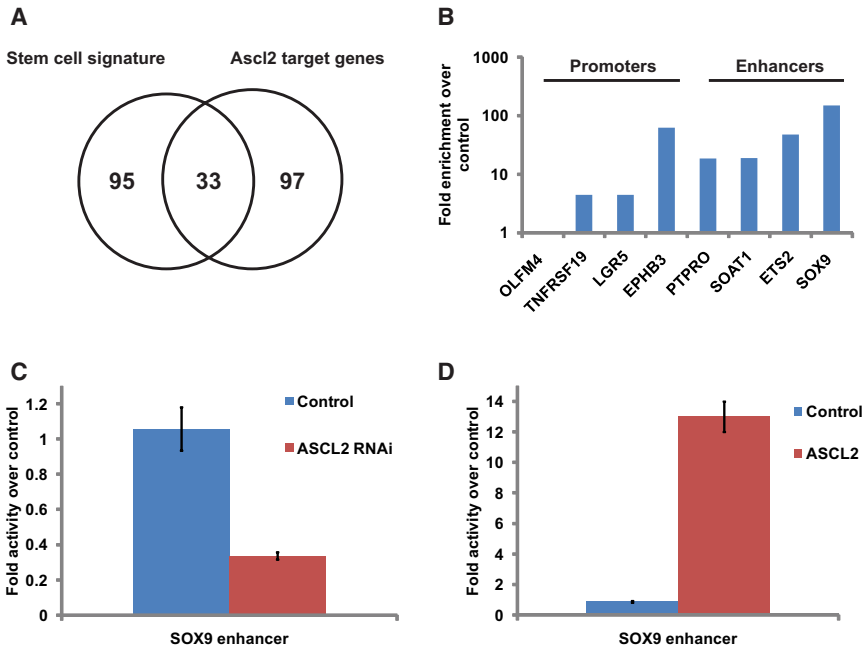

Figure 7. Ascl2 Target Genes

(A) Venn diagram showing the overlap between the stem cell signature (Table S1) and the Ascl2 target genes. Ascl2 target genes have been identified through comparative gene profiling of RNA samples from isolated intestinal epithelium of *Ah-Cre/Ascl2*$^{floxed/floxed}$ animals and *Ah-Cre/Ascl2*$^{floxed/wt}$ control animals at day 3 and 5 days PI. For the comparison of the stem cell genes and the Ascl2 target genes only those genes expressed in both lists were compared. The identity of the overlapping genes is given in Table S2.

(B) Association of ASCL2 with the proximal promoters and enhancers of the indicated Ascl2 target genes. ASCL2 binding to indicated regions is expressed as relative enrichment of the respective qPCR product over the qPCR product of the nonbound exon2 of the myoglobin gene. Experiments have been performed at least three times. A representative experiment is shown.

(C) Transcriptional activity of SOX9 enhancer in integrated inducible ASCL2 RNAi LS174T cell line. Luciferase reporter containing the SOX9 enhancer was transiently transfected in the LS174T ASCL2 RNAi cell line. A CMV-Renilla reporter was cotransfected as a normalizing control. Cells were induced for 24 hr with doxycycline to induce the sh-RNA against ASCL2. Control and ASCL2 RNAi values are normalized over the empty pGL4.10 TATA construct. Experiments have been performed at least three times. A representative experiment is shown. Values are the average of normalized triplicates and error bars represent standard deviations of these triplicates.

(D) Transcriptional activity of SOX9 enhancer in stably integrated inducible ASCL2 HCT116 cell line. Luciferase reporter containing the SOX9 enhancer was transiently transfected in inducible ASCL2 HCT116 CRC cell line. A CMV-Renialla reporter was cotransfected as a normalizing control. Cells were induced for 24 hr with doxycycline to induce ASCL2 expression. Control and ASCL2 induction values are normalized over the empty pGL4.10 TATA construct. Experiments have been performed at least three times. A representative experiment is shown. Values are the average of normalized triplicates and error bars represent standard deviations of these triplicates.

generate *Ah-Cre/Ascl2*$^{floxed/floxed}$ mice. The Cre enzyme was induced in mice 6-12 weeks old of age by intraperitoneal injections at day 0 of 200 μl β-naphthoflavone (10 mg ml^{-1}; Sigma Aldrich) dissolved in corn oil.

Isolation of Intestinal Cells for Southern and Northern Blot Analysis

Intestines were cut into small pieces and washed in ice-cold PBS (Mg^{2+}/Ca^{2+}). The intestinal pieces were incubated in 30 mM EDTA in PBS at 37 degrees followed by shaking. The released epithelium was then collected to prepare DNA or RNA by standard procedures.

Histology, Immunohistochemistry, and In Situ Hybridization

Tissues were fixed in 10% formalin, paraffin embedded, and sectioned. Antibodies: anti-Ki67 (1:100; Novacastra), rabbit anti-c-Myc (1:500; Upstate Biotechnology), mouse anti-Ascl2 (1:5; Supplemental Experimental Procedures), rabbit anti-Sox9 (1:600, Chemicon), rabbit anti-Caspase-3 (1:400; Cell signaling), rabbit anti-GFP (1:6000, gift from E. Cuppen). Peroxidase conjugated secondary antibodies used were Mouse or Rabbit EnVision+ (DAKO). Mouse ESTs were from RZPD. Protocols for in vitro transcription and in situ hybridizations are described elsewhere (Gregorieff et al., 2005). β-galactosidase (LacZ) staining was done as described previously (Barker et al., 2007).

Electron Microscopy Analysis

Tissues were fixed in 2.5% glutaraldehyde + 2.0% paraformaldehyde in cacodylate-buffer, postfixed in 1% OsO4, stained en bloced with uranylacetate, and embedded in Epon resin. The samples were examined with a Phillips CM10 microscope (Eindhoven, The Netherlands).

Generation of Transfected Cell Lines

T-Rex system (Invitrogen) was used to generate a clonal ASCL2- inducible HCT116 cell line as described previously (van de Wetering et al., 2002). LS174T cells were used to generate a clonal stable, inducible ASCL2 shRNA cell line using the pTER system as described previously (van de Wetering et al., 2003). Oligonucleotides: Table S3.

ChIP, qPCR, and Reporter Assays

ChIP, qPCR, and Reporter array protocols were performed as described previously (Hatzis et al., 2008) with small modifications. Detailed information is available in Supplemental Experimental Procedures.

ACCESSION NUMBERS

Microarray data have been deposited in the Gene Expression Omnibus Database with the accession number GSE14201.

SUPPLEMENTAL DATA

Supplemental Data include Supplemental Experimental Procedures, three tables, five figures, and Supplemental References and can be found with this article online at http://www.cell.com/supplemental/S0092-8674(09)00079-8.

ACKNOWLEDGMENTS

We would like to thank Robert Vries, Jeroen Korving, Miranda Cozijnsen, Stieneke van den Brink, Eveline Steine, Nico Ong and Marius van den Bergh Weerman for technical help. Maarten Van Lohuizen is thanked for providing Bmi1 knockout tissues. P.H. is supported by successive EMBO and HFSP fellowships.

Received: July 29, 2008
Revised: November 7, 2008
Accepted: January 7, 2009
Published: March 5, 2009

REFERENCES

Barker, N., van de Wetering, M., and Clevers, H. (2008). The intestinal stem cell. Genes Dev. *22*, 1856–1864.

Barker, N., van Es, J.H., Kuipers, J., Kujala, P., van den Born, M., Cozijnsen, M., Haegebarth, A., Korving, J., Begthel, H., Peters, P.J., and Clevers, H. (2007). Identification of stem cells in small intestine and colon by marker gene Lgr5. Nature *449*, 1003–1007.

Bastide, P., Darido, C., Pannequin, J., Kist, R., Robine, S., Marty-Double, C., Bibeau, F., Scherer, G., Joubert, D., Hollande, F., et al. (2007). Sox9 regulates cell proliferation and is required for Paneth cell differentiation in the intestinal epithelium. J. Cell Biol. *178*, 635–648.

Bjerknes, M., and Cheng, H. (1981a). The stem-cell zone of the small intestinal epithelium. I. Evidence from Paneth cells in the adult mouse. Am. J. Anat. *160*, 51–63.

Bjerknes, M., and Cheng, H. (1981b). The stem-cell zone of the small intestinal epithelium. III. Evidence from columnar, enteroendocrine, and mucous cells in the adult mouse. Am. J. Anat. *160*, 77–91.

Bjerknes, M., and Cheng, H. (1999). Clonal analysis of mouse intestinal epithelial progenitors. Gastroenterology *116*, 7–14.

Blache, P., van de Wetering, M., Duluc, I., Domon, C., Berta, P., Freund, J.N., Clevers, H., and Jay, P. (2004). SOX9 is an intestine crypt transcription factor, is regulated by the Wnt pathway, and represses the CDX2 and MUC2 genes. J. Cell Biol. *166*, 37–47.

Cabrera, C.V., and Alonso, M.C. (1991). Transcriptional activation by heterodimers of the achaete-scute and daughterless gene products of Drosophila. EMBO J. *10*, 2965–2973.

Cairnie, A.B., and Millen, B.H. (1975). Fission of crypts in the small intestine of the irradiated mouse. Cell Tissue Kinet. *8*, 189–196.

Calleja, M., Renaud, O., Usui, K., Pistillo, D., Morata, G., and Simpson, P. (2002). How to pattern an epithelium: lessons from achaete-scute regulation on the notum of Drosophila. Gene *292*, 1–12.

Caudy, M., Vassin, H., Brand, M., Tuma, R., Jan, L.Y., and Jan, Y.N. (1988). daughterless, a Drosophila gene essential for both neurogenesis and sex determination, has sequence similarities to myc and the achaete-scute complex. Cell *55*, 1061–1067.

Cheng, H., and Leblond, C.P. (1974a). Origin, differentiation and renewal of the four main epithelial cell types in the mouse small intestine. I. Columnar cell. Am. J. Anat. *141*, 461–479.

Cheng, H., and Leblond, C.P. (1974b). Origin, differentiation and renewal of the four main epithelial cell types in the mouse small intestine. V. Unitarian Theory of the origin of the four epithelial cell types. Am. J. Anat. *141*, 537–561.

Fevr, T., Robine, S., Louvard, D., and Huelsken, J. (2007). Wnt/beta-catenin is essential for intestinal homeostasis and maintenance of intestinal stem cells. Mol. Cell. Biol. *27*, 7551–7559.

Gregorieff, A., and Clevers, H. (2005). Wnt signaling in the intestinal epithelium: from endoderm to cancer. Genes Dev. *19*, 877–890.

Gregorieff, A., Pinto, D., Begthel, H., Destree, O., Kielman, M., and Clevers, H. (2005). Expression pattern of Wnt signaling components in the adult intestine. Gastroenterology *129*, 626–638.

Guillemot, F., Caspary, T., Tilghman, S.M., Copeland, N.G., Gilbert, D.J., Jenkins, N.A., Anderson, D.J., Joyner, A.L., Rossant, J., and Nagy, A. (1995). Genomic imprinting of Mash2, a mouse gene required for trophoblast development. Nat. Genet. *9*, 235–242.

Guillemot, F., Nagy, A., Auerbach, A., Rossant, J., and Joyner, A.L. (1994). Essential role of Mash-2 in extraembryonic development. Nature *371*, 333–336.

Hatzis, P., van der Flier, L.G., van Driel, M.A., Guryev, V., Nielsen, F., Denissov, S., Nijman, I.J., Koster, J., Santo, E.E., Welboren, W., et al. (2008). Genome-wide pattern of TCF7L2/TCF4 chromatin occupancy in colorectal cancer cells. Mol. Cell. Biol. *28*, 2732–2744.

Hughes, M., Dobric, N., Scott, I.C., Su, L., Starovic, M., St-Pierre, B., Egan, S.E., Kingdom, J.C., and Cross, J.C. (2004). The Hand1, Stra13 and Gcm1 transcription factors override FGF signaling to promote terminal differentiation of trophoblast stem cells. Dev. Biol. *271*, 26–37.

Inomata, H., Haraguchi, T., and Sasai, Y. (2008). Robust stability of the embryonic axial pattern requires a secreted scaffold for chordin degradation. Cell *134*, 854–865.

Ireland, H., Kemp, R., Houghton, C., Howard, L., Clarke, A.R., Sansom, O.J., and Winton, D.J. (2004). Inducible Cre-mediated control of gene expression in the murine gastrointestinal tract: effect of loss of beta-catenin. Gastroenterology *126*, 1236–1246.

Johnson, J.E., Birren, S.J., and Anderson, D.J. (1990). Two rat homologues of Drosophila achaete-scute specifically expressed in neuronal precursors. Nature *346*, 858–861.

Johnson, J.E., Birren, S.J., Saito, T., and Anderson, D.J. (1992). DNA binding and transcriptional regulatory activity of mammalian achaete-scute homologous (MASH) proteins revealed by interaction with a muscle-specific enhancer. Proc. Natl. Acad. Sci. USA *89*, 3596–3600.

Jubb, A.M., Chalasani, S., Frantz, G.D., Smits, R., Grabsch, H.I., Kavi, V., Maughan, N.J., Hillan, K.J., Quirke, P., and Koeppen, H. (2006). Achaete-scute like 2 (ascl2) is a target of Wnt signalling and is upregulated in intestinal neoplasia. Oncogene *25*, 3445–3457.

Korinek, V., Barker, N., Moerer, P., van Donselaar, E., Huls, G., Peters, P.J., and Clevers, H. (1998). Depletion of epithelial stem-cell compartments in the small intestine of mice lacking Tcf-4. Nat. Genet. *19*, 379–383.

Korinek, V., Barker, N., Morin, P.J., van Wichen, D., de Weger, R., Kinzler, K.W., Vogelstein, B., and Clevers, H. (1997). Constitutive transcriptional activation by a beta-catenin-Tcf complex in APC−/− colon carcinoma. Science *275*, 1784–1787.

Kosinski, C., Li, V.S., Chan, A.S., Zhang, J., Ho, C., Tsui, W.Y., Chan, T.L., Mifflin, R.C., Powell, D.W., Yuen, S.T., et al. (2007). Gene expression patterns of human colon tops and basal crypts and BMP antagonists as intestinal stem cell niche factors. Proc. Natl. Acad. Sci. USA *104*, 15418–15423.

Kuhnert, F., Davis, C.R., Wang, H.T., Chu, P., Lee, M., Yuan, J., Nusse, R., and Kuo, C.J. (2004). Essential requirement for Wnt signaling in proliferation of adult small intestine and colon revealed by adenoviral expression of Dickkopf-1. Proc. Natl. Acad. Sci. USA *101*, 266–271.

Mori-Akiyama, Y., van den Born, M., van Es, J.H., Hamilton, S.R., Adams, H.P., Zhang, J., Clevers, H., and de Crombrugghe, B. (2007). SOX9 is required for the differentiation of paneth cells in the intestinal epithelium. Gastroenterology *133*, 539–546.

Morin, P.J., Sparks, A.B., Korinek, V., Barker, N., Clevers, H., Vogelstein, B., and Kinzler, K.W. (1997). Activation of beta-catenin-Tcf signaling in colon cancer by mutations in beta-catenin or APC. Science *275*, 1787–1790.

Muncan, V., Sansom, O.J., Tertoolen, L., Phesse, T.J., Begthel, H., Sancho, E., Cole, A.M., Gregorieff, A., de Alboran, I.M., Clevers, H., and Clarke, A.R. (2006). Rapid loss of intestinal crypts upon conditional deletion of the Wnt/Tcf-4 target gene c-Myc. Mol. Cell. Biol. *26*, 8418–8426.

Phillips, R.G., and Whittle, J.R. (1993). wingless expression mediates determination of peripheral nervous system elements in late stages of Drosophila wing disc development. Development *118*, 427–438.

Pinto, D., Gregorieff, A., Begthel, H., and Clevers, H. (2003). Canonical Wnt signals are essential for homeostasis of the intestinal epithelium. Genes Dev. *17*, 1709–1713.

Pinto, D., Robine, S., Jaisser, F., El Marjou, F.E., and Louvard, D. (1999). Regulatory sequences of the mouse villin gene that efficiently drive transgenic expression in immature and differentiated epithelial cells of small and large intestines. J. Biol. Chem. *274*, 6476–6482.

Potten, C.S. (1977). Extreme sensitivity of some intestinal crypt cells to X and gamma irradiation. Nature *269*, 518–521.

Potten, C.S., Kovacs, L., and Hamilton, E. (1974). Continuous labelling studies on mouse skin and intestine. Cell Tissue Kinet. *7*, 271–283.

Reya, T., and Clevers, H. (2005). Wnt signalling in stem cells and cancer. Nature *434*, 843–850.

Sangiorgi, E., and Capecchi, M.R. (2008). Bmi1 is expressed in vivo in intestinal stem cells. Nat. Genet. *40*, 915–920.

Sansom, O.J., Reed, K.R., Hayes, A.J., Ireland, H., Brinkmann, H., Newton, I.P., Batlle, E., Simon-Assmann, P., Clevers, H., Nathke, I.S., et al. (2004). Loss of Apc in vivo immediately perturbs Wnt signaling, differentiation, and migration. Genes Dev. *18*, 1385–1390.

Scott, I.C., Anson-Cartwright, L., Riley, P., Reda, D., and Cross, J.C. (2000). The HAND1 basic helix-loop-helix transcription factor regulates trophoblast differentiation via multiple mechanisms. Mol. Cell. Biol. *20*, 530–541.

Simpson, P. (1990). Lateral inhibition and the development of the sensory bristles of the adult peripheral nervous system of Drosophila. Development *109*, 509–519.

Soriano, P. (1999). Generalized lacZ expression with the ROSA26 Cre reporter strain. Nat. Genet. *21*, 70–71.

van de Wetering, M., Oving, I., Muncan, V., Pon Fong, M.T., Brantjes, H., van Leenen, D., Holstege, F.C., Brummelkamp, T.R., Agami, R., and Clevers, H. (2003). Specific inhibition of gene expression using a stably integrated, inducible small-interfering-RNA vector. EMBO Rep. *4*, 609–615.

van de Wetering, M., Sancho, E., Verweij, C., de Lau, W., Oving, I., Hurlstone, A., van der Horn, K., Batlle, E., Coudreuse, D., Haramis, A.P., et al. (2002). The beta-catenin/TCF-4 complex imposes a crypt progenitor phenotype on colorectal cancer cells. Cell *111*, 241–250.

van der Flier, L.G., Sabates-Bellver, J., Oving, I., Haegebarth, A., De Palo, M., Anti, M., Van Gijn, M.E., Suijkerbuijk, S., Van de Wetering, M., Marra, G., and Clevers, H. (2007). The Intestinal Wnt/TCF Signature. Gastroenterology *132*, 628–632.

van der Lugt, N.M., Domen, J., Linders, K., van Roon, M., Robanus-Maandag, E., te Riele, H., van der Valk, M., Deschamps, J., Sofroniew, M., van Lohuizen, M., et al. (1994). Posterior transformation, neurological abnormalities, and severe hematopoietic defects in mice with a targeted deletion of the bmi-1 proto-oncogene. Genes Dev. *8*, 757–769.

van Es, J.H., Jay, P., Gregorieff, A., van Gijn, M.E., Jonkheer, S., Hatzis, P., Thiele, A., van den Born, M., Begthel, H., Brabletz, T., et al. (2005). Wnt signalling induces maturation of Paneth cells in intestinal crypts. Nat. Cell Biol. *7*, 381–386.

Zhang, J., Liu, W.L., Tang, D.C., Chen, L., Wang, M., Pack, S.D., Zhuang, Z., and Rodgers, G.P. (2002). Identification and characterization of a novel member of olfactomedin-related protein family, hGC-1, expressed during myeloid lineage development. Gene *283*, 83–93.